Waste and Biomass Valorization (2022) 13:173–183
https://doi.org/10.1007/s12649-021-01495-x

ORIGINAL PAPER

Preparation and Characterization of a Novel Nanocellulose-Derivative as a Potential Radiopharmaceutical Agent

Lecot Nicole[1] · Gandaras Rosario[1,2] · Batista-Menezes Diego[3] · Montes de Oca-Vásquez Gabriela[3] · Cabral Pablo[4] · García Ma. Fernanda[4] · Vega-Baudrit José[3,5] · Cerecetto Hugo[2,4] · Lopretti Mary[1]

Received: 28 November 2020 / Accepted: 26 April 2021 / Published online: 23 June 2021

Abstract

Nanocellulose (NC) has a wide variety of emerging applications, including enzyme immobilization, drug delivery, and imaging diagnosis. On the other hand, derivatives of hydrazinonicotinic acid (HYNIC) have been used as coordination-agents for their binding to ^{99m}Tc in the development of potential radiopharmaceuticals. To this end, we studied and developed NC-HYNIC-^{99m}Tc for diagnostic imaging using NC obtained from rice husk using *Trichoderma reseii* and *Phanaerochaete chrysosporium* in a semi-solid fermentation system to generate a potential nanoradiopharmaceutical agent. In this work, we performed the separation of nanosilica, microcellulose, and nanocellulose using the TAPPI T203 os-74 technique. The synthesis of conjugate NC-HYNIC was performed following a one-pot procedure. The NC and the conjugate NC-HYNIC were characterized by Fourier Transform Infrared Spectroscopy (FTIR), thermogravimetric analysis (TGA), scanning electron microscopy (SEM), and atomic force microscopy (AFM). We obtained NC with a structure of laminar-like nanofibers. The yield of NC was 55% and the conjugate NC-HYNIC was obtained with a yield of 36%. The TGA and FTIR analyses showed that the NC functionalized with HYNIC had similar characteristics to those of NC. In addition, the AFM analysis of the functionalized NC showed an average height of 8 ± 3 nm, while the NC showed an average height of 10 ± 4 nm. The subsequent binding to ^{99m}Tc was assayed, and the purity of the radiolabeled product and the efficiency of the process was studied by ITLC chromatography. The radiolabeling process was very efficient with a radiochemical purity of 98 ± 1.2%, which opens the possibility of a new potential-imaging agent.

Graphic Abstract

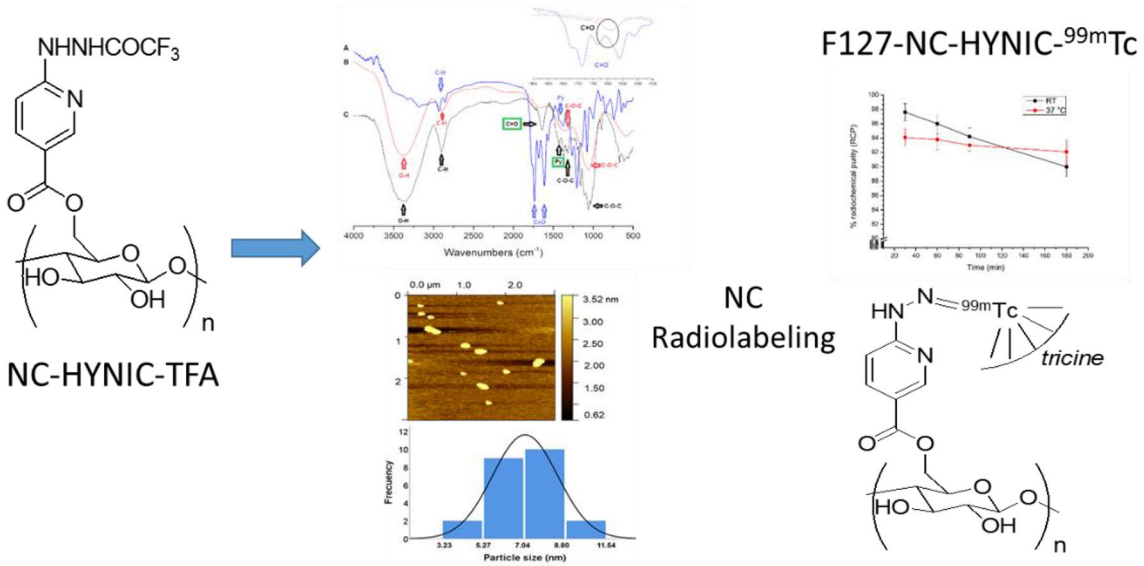

Extended author information available on the last page of the article

Keywords Biomass valorization · Nanocellulose · Nanocellulose functionalization · ^{99m}Tc-nanoradiotracer

Statement of Novelty

Rice husk represents an abundant waste and currently has limited uses due to its composition, having negative effects on the environment by its slow biodegradation rate. We studied the valorization of rice husk as a source of nanocellulose in a semi-solid fermentation system and its functionalization with hydrazinonicotinyl moiety. This new strategy of radiolabeled nanocellulose demonstrates a promising application of F127-nanocellulose-HYNIC-^{99m}Tc as a nanoradiopharmaceutical agent according to its high radiolabeling yield and stability.

Introduction

Nowadays, there is a great amount of waste derived from renewable bio-resources, which could be an alternative to replace petroleum-based products due to their advantages, such as easy availability, environmental friendliness, and relatively low cost [1, 2]. Cellulose, considered one of the most important natural resources, is non-toxic and it is the most abundant and renewable natural polymer on the Earth [2, 3].

Rice husk (RH), a residue produced by the rice industry in large quantities, has been a substantial problem because of the limited reuse it currently has due to its composition, which consists of cellulose-based fibers and minerals with long biodegradation times and high toxicity [4]. However, several processes could use RH waste as a raw material to generate high added-value products with multiple industrial applications [5, 6]. RH has been described as a source of silica, silicon compounds, xylitol, furfural, ethanol, acetic acid, nanoparticles, bioethanol production, flexible foams, and nanocellulose [4, 5, 7–9].

Nanocellulose (NC) is a renewable, biodegradable, and relatively inexpensive polymer of high aspect ratio and surface area [3, 10–12]. It has been reported as a potential agent for enzyme immobilization, drug delivery application, diagnostic imaging, and other biomedical uses [13, 14]. In this sense, NC has become a new class of nanomaterial for polymer reinforcement and nanoformulation [15] due to its exceptional characteristics. Among its properties, NC exhibits high mechanical resistance (100–140 GPa young's modulus), low density (1.6 g cm^{-3}), environmental sustainability, and low aqueous solubility, while also constituting a non-toxic, biodegradable, renewable, low-cost, and chemically-modifiable material [4, 16]. It can be extracted from cellulose from various raw materials by using different methods, including chemical, physical, and biological treatments [17]. However, the main extraction methods are acid hydrolysis, enzymatic hydrolysis, and mechanical processes [12].

Thus, we propose to produce NC by a semi-solid fermentation process using *Trichoderma reseii* and *Phanaerochaete chrysosporium* [18, 19]. The biological treatment using microorganisms via an enzymatic reaction is a green process [20] that could incorporate other methods such as pretreatments to shorten process times [12]. Different types of polymeric micelles have been used as solubilizers or surfactants of different poorly soluble molecules [21–23]. Particularly, F127 poloxamers form spherical amphiphilic copolymers with low critical micelle concentration (CMC), providing a platform for the solubilization and the delivery of nanostructures like NC derivatives as molecular diagnostic agents.

Furthermore, 99-metastable technetium (^{99m}Tc) is one of the most used among the diagnostic radionuclides employed in medicine to prepare radiopharmaceuticals [24, 25] for molecular imaging by scintigraphic techniques. ^{99m}Tc has attractive characteristics such as nuclear decay, polyvalent redox chemistry, and widespread clinical utility [26]. In addition, the 6-hydrazinonicotinic acid (HYNIC) agent and its derivatives were well reported as efficient bifunctional chelators of ^{99m}Tc, binding to a variety of biomolecules such as peptides and proteins for molecular imaging [27, 28]. The use of ^{99m}Tc-HYNIC derivatives has been extensively described for the detection of tumors, infections, and inflammatory diseases [29, 30]. However, to date only few studies have reported the use of NC and ^{99m}Tc for diagnostic imaging [31, 32]. In this sense, herein we propose the development and use of NC-HYNIC-^{99m}Tc for diagnostic imaging through the binding of NC to a derivative of HYNIC which is able to coordinate with metals like ^{99m}Tc.

Experimental Methods

Trichoderma reseii and *Phanaerochaete chrysosporium* Pre-Inoculum

The microorganisms (*Trichoderma reseii* and *Phanaerochaete chrysosporium*) were cultured separately, each ina Yeast Extract Peptone Dextrose broth (YPD) medium (10 g/L of distilled water) at 37 °C for 10 days. The two strains were cultured separately to be able to inoculate the RH at time zero of the semi-solid fermentation (SSF) system, and with *Trichoderma reseii* at 5 days of fermentation in the SSF system to perform the polymer transformation and depolymerization.

Nanocellulose (NC) Extraction from Rice Husk

The material to obtain NC from RH was provided by the Uruguayan rice production company SAMAN S.A. in 2-kg bags at the port of Montevideo, Uruguay, without having gone through any stage of purification.

NC was obtained from RH by means of a biologic method using a microscale-up technique with some modifications to the SSF system [18, 19]. The SSF assay took place in a wetted column system (20 mL) (Rainbow system) [33, 34], with five pellets of *Trichoderma reseii* and five pellets of *Phanaerochaete chrysosporium* pre inoculum (experimental methods 2.1), during 40 days at 37 °C. Samples obtained by SSF at a humidity of 60% and pH = 5 were taken every 7 days by leaching with sterile water until the time of fermentation, with the subsequent separation and quantification of the nanosilica, the microcellulose, and the nanocellulose performed by the TAPPI T203 os-74 technique [35]. Sterile samples were dried in a stove at 40 °C for 10 days and were used for characterization analysis and further functionalization without further treatment.

The NC yield was determined from the mass of the nanocellulose suspension obtained after precipitation by centrifugation at 15,000 rpm for 10 min and drying to constant mass in an oven at 50 °C. The NC yield was calculated according to the following relation [36]:

$$\text{Yield of NC (\%)} = (\text{g of dried mass (NC)}/\text{g of MSS}) \times 100$$

MSS: grams of RH that was initially used to extract the NC.

Synthesis of Conjugate NC-HYNIC (NC-HYNIC-TFA)

The synthesis of NC-HYNIC-TFA was developed according to the bibliography with slight modifications [37–41]. NC (4 mg) was briefly suspended in *N,N*-dimethylformamide (DMF, 0.5 mL), and subsequently ultrasonicated at 400 W for 5 min [42, 43] in a water bath to avoid the overheating of NC. Then, triethylamine (0.05 mL) and 6-(2-trifluoroacetylhydrazinyl) nicotinic acid *N*-hydroxysuccinimide (NHS-HYNIC-TFA, 2.5 mg) were added [44]. The reaction was stirred for 16 h at room temperature. After that, the solid was filtered off and the solid residue was washed with DMF (10 mL). Finally, the system was centrifuged at 9500 rpm for 11 min. After centrifugation, the supernatant was discarded and the pellet was washed twice with ethanol (via additional centrifugations), followed by two additional washes and centrifugation with water. Once the washings were performed, the obtained solid product, NC-HYNIC-TFA, was lyophilized and stored at 4 °C for further characterization and experiments. The yield of NC-HYNIC-TFA was calculated based on the isolated and dried final product from the reaction milieu (n = 3).

Characterization of NC and NC-HYNIC-TFA

Fourier Transformed Infrared Spectroscopy Analysis

The samples were ground in a mill and the powders were pressured with KBr (Sigma Aldrich). The analysis was done by FTIR in a Nicolet spectrophotometer 6700 (Thermo Scientific), using an ATR accessory with a diamond crystal. The analyses were performed in triplicate. FTIR spectra of NC and NC-HYNIC-TFA were performed on each sample in attenuated total reflectance mode (4000–500 cm^{-1}) and 16 scans were of 4 cm^{-1} of resolution on average.

Thermogravimetric Analysis

The TGA of NC and NC-HYNIC-TFA were performed using TGA Q500 equipment (TA Instruments, USA), and the Universal Analysis 2000 software (version 4.5A, TA Instruments). The analyses were performed using a temperature ramp of 10 °C/min from room temperature to 600 °C and subsequently ramped up to 20 °C/min from 600 to 1000 °C under nitrogen (flow rate of 90 mL/min). The analyses were performed in triplicate on 5–8 mg samples placed in a standard platinum pan.

Scanning Electron Microscopy

The morphology of NC and NC-HYNIC-TFA was metalized with a thin layer of gold by sputtering in a Denton Vacuum Desk V at 20 mA with an exposure time of 5 min. The images at different magnifications were taken using a JEOL scanning electron microscope (model JSM-6390LV), with an acceleration voltage of 15 kV, detecting secondary electrons (SEI) with a spot size of 50. The representative images of NC and NC-HYNIC-TFA were reported in 5 regions of three independent samples.

Atomic Force Microscopy

The height and frequency of three independent samples of NC and NC-HYNIC-TFA were imaged with an Asylum Research microscope (MFP-3D AFM). A drop of the samples in suspension was placed into a mica substrate and was allowed to air dry at room temperature (23 °C) for 24 h. Samples were analyzed via tapping mode AFM using a Nanosurf Dyn190Al probe with a resonant frequency of f_0 = 190 kHz (160–220 kHz) and a stiffness of k = 48 N/m (28–75 N/m). Histograms from NC and NC-HYNIC-TFA were performed using IBM SPSS (version 20.0; SPSS Inc, Chicago, IL, USA).

Radiolabeling of NC-HYNIC-TFA

Preparation of F127-NC-HYNIC-TFA Polymeric Micelles

The NC-HYNIC-TFA polymeric micelles (PMs) were prepared using a self-assembly method in an aqueous solution [23]. Briefly, Pluronic F127 and NC-HYNIC-TFA (95:5, w/w) were hydrated in Milli-Q water at 4 °C for 45 min. The NC-HYNIC-TFA was completely solubilized by stirring at 200 rpm for 1 h at 25 °C. Lastly, NC-HYNIC-TFA PMs and F127-NC-HYNIC-TFA were filtered in 0.22 µm polycarbonate membranes and were used without any further purification [45].

Radiolabeling and Radiochemical Stability of F127-NC-HYNIC-^{99m}Tc

Tricine coligand (7 mg, Sigma-Aldrich, USA) was dissolved in saline solution (NaCl solution 0.9%, 0.8 mL). The pH was adjusted to 4.5–5.0 with an aqueous solution of hydrochloric acid (1.0 M, 0.05 mL) and a saline solution was added to complete 1.0 mL (solution A). In a second vial, $SnCl_2.2H_2O$ (6 mg, J. T. Baker, USA) was dissolved in ethanol (EtOH, 0.5 mL) and 0.05 mL of this solution was added to solution A [46] as a reducing agent. Finally, the volume was adjusted to 1.0 mL with a saline solution (solution B). Afterwards, F127-NC-HYNIC-TFA (400 µL) was radiolabeled by mixing it with solution B (100 µL) and $Na^{99m}TcO_4$ (130–185 MBq, ^{99}Mo-^{99m}Tc generators, TecnoNuclear, Argentina) (300–400 µL). The mixtures were incubated at room temperature for 20 min. Lastly, the mixture of the reaction was filtered through 0.22 µm polycarbonate membranes to eliminate the $^{99m}TcO_2$ impurity [47, 48].

The radiochemical purity (RCP) of F127-NC-HYNIC-^{99m}Tc was established by ascending an instant thin-layer chromatography (ITLC-SG (Pall Corporation, USA) and Whatman 1 (W1) (Sigma Aldrich, USA), using the chromatographic mobile phase systems of saline/W1, acetone/ITLC-SG, and 2-butanone/W1. After that, the strips were air-dried and cut in 6–8 segments. The activity was counted in a CRC7 Capintec dose calibrator (Mirion Technologies, USA) and in a solid scintillation counter detector with a 3″×3″ NaI(Tl) crystal associated with a single channel analyzer (ORTEC, Oak Ridge, TN) [48, 49].

Radiochemical stability in the reaction milieu (saline solution at 25 °C) was determined from samples (100 uL, 3–4.2 MBq) collected at 30, 60, 90, and 180 min after the radiolabeling of three independent F127-NC-HYNIC-^{99m}Tc fresh solutions. The radiochemical stability in mouse serum was done by the incubation of F127-NC-HYNIC-99mTc (fresh solutions, 100 uL, 3–4.2 MBq) in 900 µL of mouse serum up to 3 h at 37 °C. Proteins were precipitated with 100 µL of anhydrous acetonitrile, shaken on a vortex and centrifuged at 1000 g for 5 min (4 °C) [49, 50]. The RCP in both milieus (reaction milieu and mouse serum) were evaluated through chromatography systems previously described in this work.

Results

Nanocellulose (NC) Extraction from Rice Husk and NC-HYNIC-TFA Synthesis

The extraction yield of NC was 55.2 ± 5.29% of the dried final product obtained (2.94 ± 0.19 g) of RH (5.02 g). NC was characterized by FTIR, TGA, and SEM analysis. The NC functionalization was performed following a one-pot procedure as schematically depicted in Fig. 1, where the C6 primary alcohol of NC [37–41] reacted with an activated HYNIC-derivative, NHS-HYNIC-TFA [25]. The yield of the NC-HYNIC-TFA synthesis was 36%. For each HYNIC-derivative, three replicate samples were analyzed.

Characterization of NC and NC-HYNIC-TFA Nanomaterials

The NC and NC-HYNIC-TFA samples were analyzed by FTIR, TGA, SEM, and AFM studies.

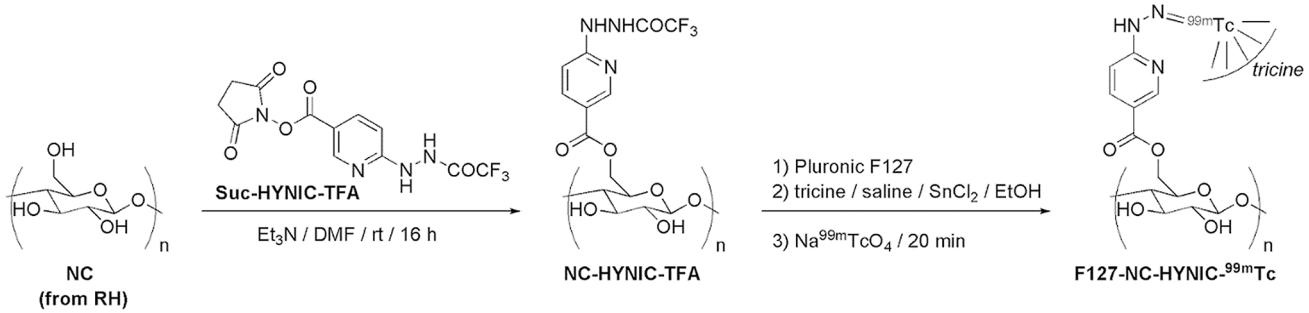

Fig. 1 Schematic procedure to obtain NC-HYNIC-TFA and the radiolabeling derivative F127-NC-HYNIC-99mTc

Fourier Transformed Infrared Spectroscopy Analysis Results

In order to determine the correct NC-functionalization, FTIR analyses of the lyophilized NHS-HYNIC-TFA, NC, and NC-HYNIC-TFA were performed (Fig. 2). Otherwise, the generated NC-HYNIC-TFA maintained, like NC, the hydroxyl stretching signals in 3200–3800 cm^{-1}, the C–H stretching vibration at region 2904 cm^{-1}, and the stretching vibration of C–O–C at 1050 cm^{-1}. The spectral peaks observed at 1379 and 1314 cm^{-1} were attributed to the twisting vibration of C–O–C and $–CH_2$ groups. Additionally, the product NC-HYNIC-TFA has new bands in the 1812–1603 cm^{-1} range, which may correspond to the stretching vibration of the carbonyl group of the ester and hydrazide, and at 1450 cm^{-1}, which may correspond to the stretching vibrations in the pyridine ring [51] functionalities incorporated in the reaction.

Thermogravimetric Analysis (TGA)

The weight-loss mass of NHS-HYNIC-TFA functionalized with NC was measured by TGA. The TGA curves of pure NHS-HYNIC-TFA, NC, and NC-HYNIC-TFA (Fig. 3a) show that the higher percentage of decomposition of NHS-HYNIC-TFA, NC, and NC-HYNIC-TFA occurred at 30–484.22 °C (77.58% wt), 160–411 (81.25% wt), and 117–303 °C (42.97% wt), respectively (Fig. 3b).

Scanning Electron Microscopy (SEM)

Figure 4 shows SEM micrographs of the NC of RH produced by enzymatic treatment (Fig. 4a) and the NC-HYNIC-TFA derivative (Fig. 4b). In image A, it is possible to observe the RH residue after the enzymatic treatment, where some cellulose nanofibers can be identified. The NC-HYNIC-TFA (Fig. 4b) images show the presence of cellulose nanofibers more clearly, probably due to physical processes during the functionalization stage. In both images, it is possible to observe the nanofibers by demarcating them with circles and red arrows (Fig. 4a and b).

Atomic Force Microscopy Analysis

AFM studies were performed in order to supplement the SEM images. The microscopies showed nanometric structures in at least one dimension (Fig. 5), with an average height of 10 ± 4 nm (n = 23) for NC and 8 ± 3 nm (n = 23) for NC-HYNIC-TFA.

Radiolabeling of NC-HYNIC-TFA

The solubility in the aqueous solution of NC and NC-HYNIC-TFA was poor; consequently, and in order to avoid this problem, we analyzed the use of a poloxamer (Pluronic F-127) as a solubilizer. These polymeric micelles

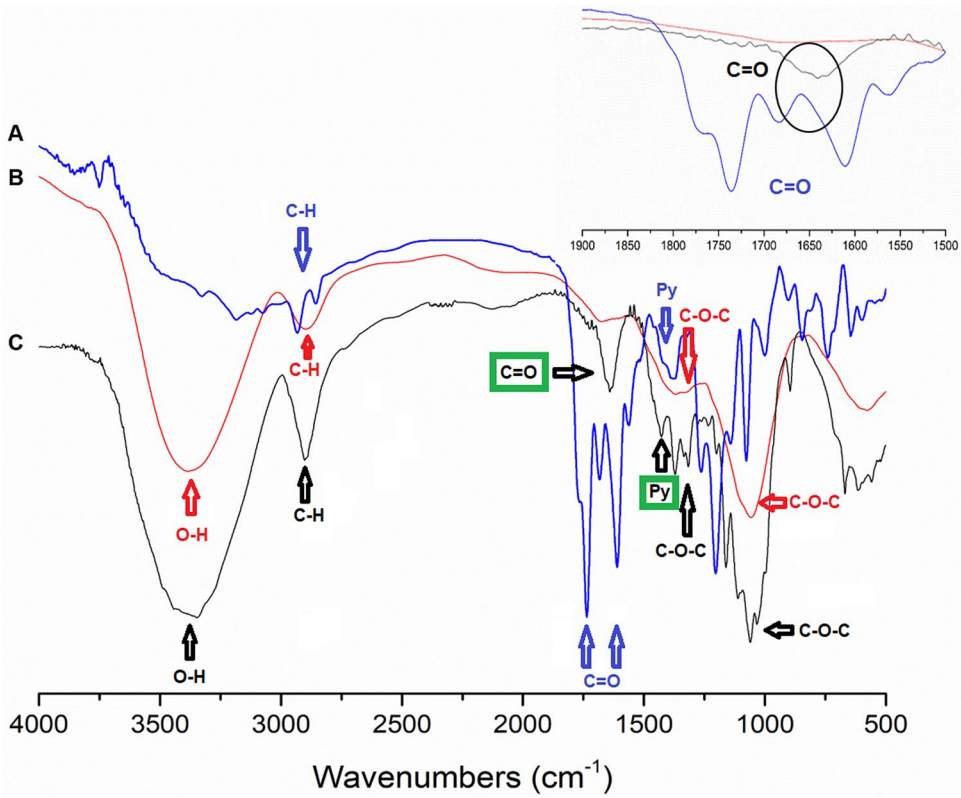

Fig. 2 FTIR spectra of Suc-HYNIC-TFA (a, blue), NC of RH (b, red), and NC-HYNICTFA (c, black). The relevant signals for Suc-HYNIC-TFA, NC of RH and NC-HYNIC-TFA are marked in blue, red and black, respectively. Green square marked new functional groups

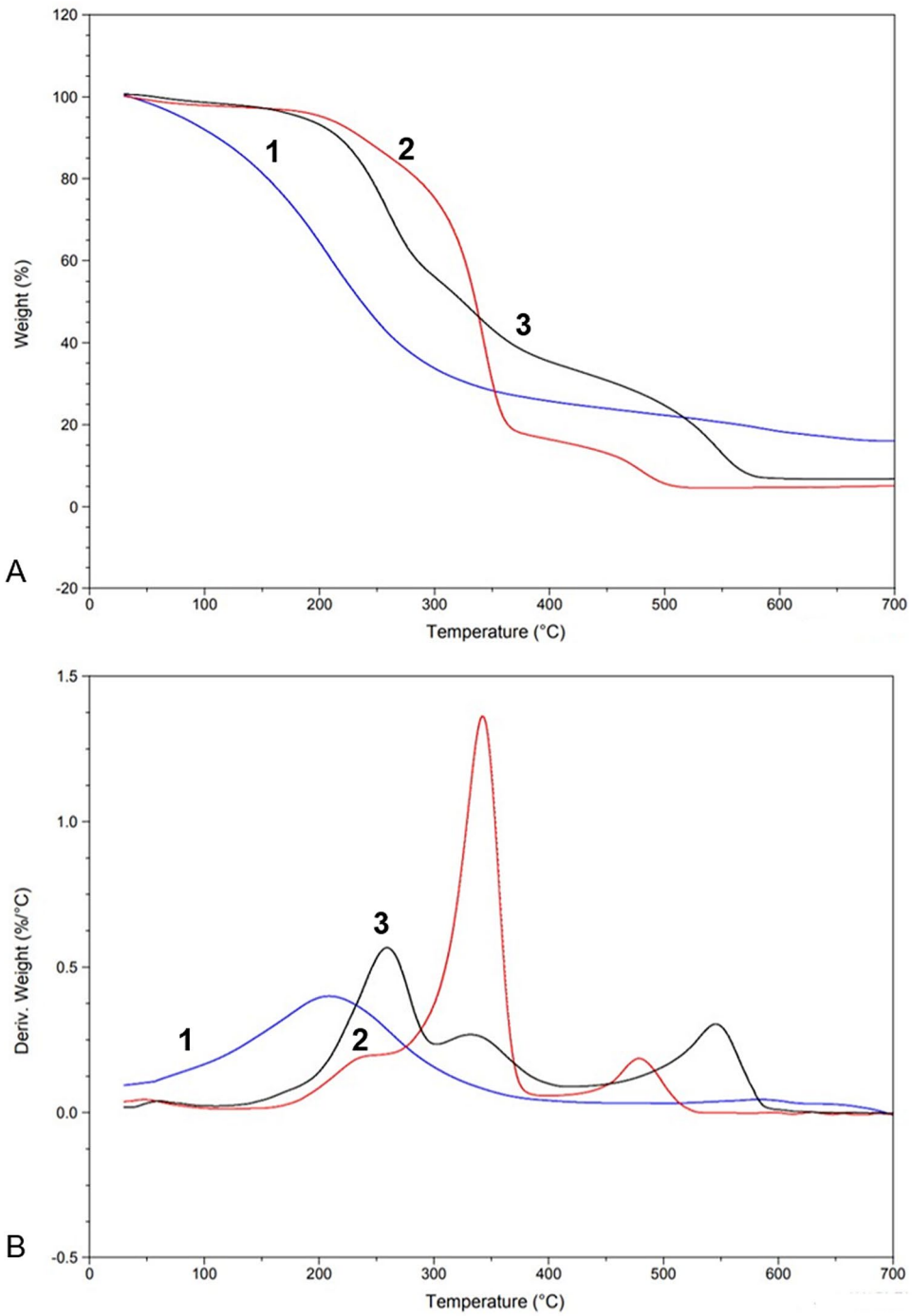

Fig. 3 Gravimetric (**a**) and differential (**b**) curve profiles of thermal analysis of Suc-HYNIC-TFA (1, blue), NC of RH (2, red), and NC-HYNIC-TFA (3, black)

allowed the partial and complete-solubilization of NC and NC-HYNIC-TFA, respectively. With these results, we assayed the F127-NC-HYNIC-TFAs radiolabeling with ^{99m}Tc following the procedure shown in Fig. 1. The pH of the radiolabeled F127-NC-HYNIC was 6.9 ± 0.3. The processes were successful at 20 min of radiolabeling, generating products with radiochemical purity higher than $98 \pm 1.2\%$. The radiolabel of F127-NC was unsuccessful in showing the relevance of the incorporation of the HYNIC-group for the correct labeling. In vitro evaluation of radiochemical stability in saline solution was determined during that time at room temperature (RT) and in the mouse serum at 37 °C, finding good stability up to a time greater than three hours (Fig. 6).

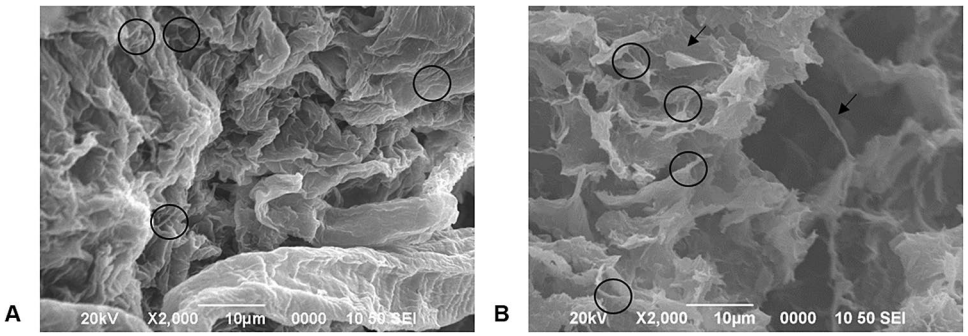

Fig. 4 Scanning electron micrographs of NC of RH (**a**) and NC-HYNIC-TFA (**b**). The circles show the cellulose nanofibers and the arrow indicates the disaggregation of laminar-like cellulose structures

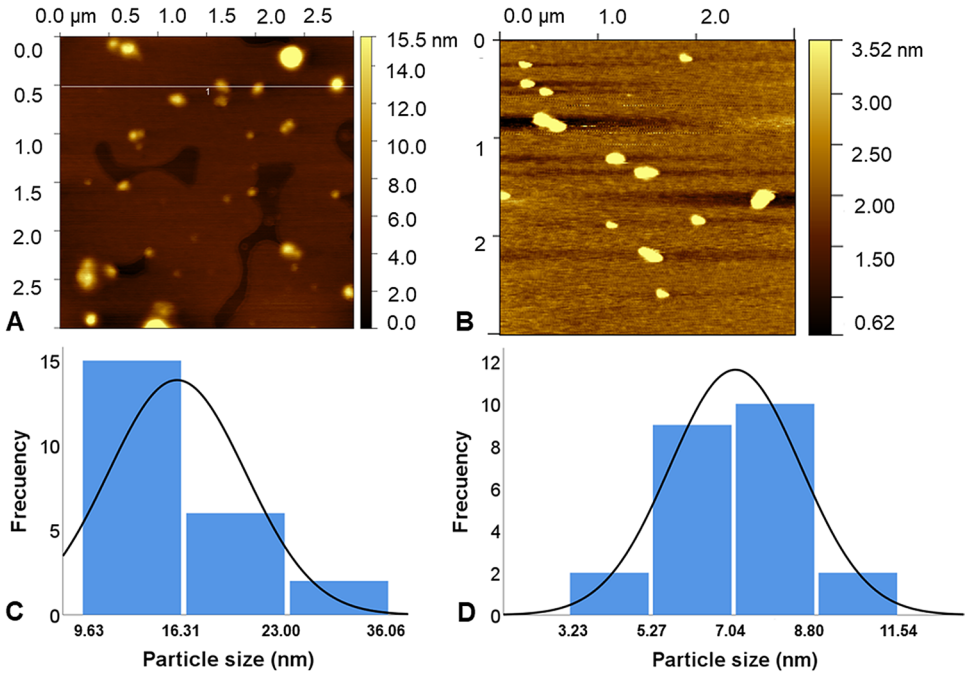

Fig. 5 AFM height images and size distribution histograms of NC (**a**, **C**) and NCHYNIC-TFA (**b**, **d**). Samples were prestabilized onto a mica substrate at 23 °C for 24 h prior to the analysis

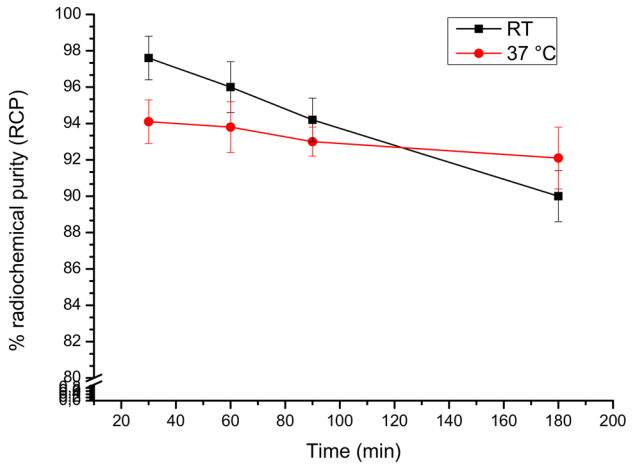

Fig. 6 Stability studies by radiochemical purity (%RCP) analysis of F127-NC-HYNIC-99mTc at different time points in reaction milieu (pH = 6.9 at room temperature) and in serum (pH = 7.0 at 37 °C). The values represent the mean of %RCP ± S.D. (n=3)

Discussion

NC is a renewable natural material, biocompatible with a nanofiber-like surface reactivity structure [11, 52]. In addition, it has been reported that NC has low toxicity and environmental risk [53], which encourages us to implement further biomedical applications. A lot of processes have been extensively used for the isolation of NC from lignocellulosic biomass, such as acid hydrolysis, enzymatic treatments, and mechanical processes [42, 53]. Among them, NC obtained through a biological transformation by a partial depolymerization and transformation of cellulose is presented as a scalable, relatively clean, and economical methodology [54, 55]. In this research, we produced NC from rice husk (RH) using *T. reesei* and *P. chrysosporium* in a semi-solid fermentation. With this methodology, the yield of extracted nanocellulose was 55%, higher than that reported in the literature [54, 55].

Satyamurthy et al. [54] produced microcrystalline cellulose using the fungus *T. reesei* and obtained a yield of 22%. Otherwise, Satyamurthy and Vigneshwaran [55] used an anaerobic microbial consortium as a source of cellulase and found that this consortium was able to produce nanocellulose for 7 days, with a maximum yield of 12.3%. *T. reesei* is used for the industrial production of lignocellulose-degrading enzymes and uses many different enzymes for the degradation of plant cell wall derived material [11, 54]. Moreover, *P. chrysosporium* belongs to a group of lignin-degrading fungi that produce oxidoreductive enzymes (lignin peroxidase and manganese peroxidase) [56–58]. It has been reported that the NC from enzymatic hydrolysis produces nanostructures that are easier to functionalize and have high thermal stability [59]. Moreover, the physicochemical properties of the NC provided a high specific surface due to the nanometric size with hydroxyl groups. The hydroxyl group enables a reaction via ester bonds with small particles [60, 61] such as HYNIC derivatives for the development of ^{99m}Tc-linked radiotracers. Therefore, controlling the type of NC synthesis process is of great importance. Otherwise, the NC obtained from RH [34] was functionalized with NHS-HYNIC-TFA with one-pot synthesis and a yield of 36% [37–41], obtaining NC-HYNIC-TFA. The characterization of both NC and NC-HYNIC-TFA was performed using different techniques such as FTIR, TGA, SEM, and AFM.

The FTIR spectra showed the presence of the relevant peaks of OH, C-O, and CH, confirming the presence of NC produced enzymatically from RH. Several studies on NC extraction from agricultural waste showed similar peaks of NC IR spectra [17, 62, 63]. The chemical bonding of HYNIC-TFA with NC was confirmed using the FTIR spectrum, showing a characteristic peak in the range of 1812–1603 cm^{-1}, which may correspond to the stretching vibration of the carbonyl group of the ester and hydrazine, and at 1450 cm^{-1}, which may correspond to the stretching vibrations in pyridine ring [51] functionalities incorporated in the reaction. These peaks did not appear in the individual FTIR spectra of NC. Otherwise, the SEM micrographs of NC showed cellulose nanofibers and laminar-like structures produced from the depolymerization process of lignocellulose matrix after the enzymatic hydrolysis of RH [33, 59, 63]. It has been reported that the NC morphology is highly dependent on the biomass source, production method, and treatment conditions, such as temperature and treatment time [64, 65]. However, the functionalized NC, NC-HYNIC-TFA, showed the presence of more cellulose nanofibrillated fibers. This could be explained by the ultrasonication process [40, 43] carried out previously the functionalization, which could disintegrate large NC aggregates and yield shorter and thinner particles [66]. This result was consistent with the AFM experiments that showed a decrease in the average height size compared to NC. Moreover, the AFM also confirmed the production of NC from RH, which had a mean size of 10 ± 4 nm of height. These observations were similar to Ludueña's reports for NC-RH using a chemical method [67] and lesser than the ones reported by Vigneshwaran and Satyamurthy [11], who found a mean size of 100 nm of thickness using acid and enzymatic hydrolysis of cotton fibers. On the other hand, Satyamurthy and Vigneshwaran et al. [55], produced nanocellulose from microcrystalline cellulose derived from cotton fibers subjected to controlled hydrolysis using an anaerobic microbial consortium, and the resultant nanocellulose had a bimodal size distribution of 43 ± 13 and 119 ± 9 nm, according to the analysis by atomic force microscopy.

The thermal experiments for NC-HYNIC-TFA indicate different temperature events of degradation compared to NC. The drying stage for all samples occurred at a temperature range of approximately 2.46–160.92 °C, which was due to the evaporation of water. Additionally, the other main weight loss (81.25%) of NC was between 160.92 and 411.92 °C related to the polymer chain scission and cross-link breakage [68]. On the other hand, according to the NC-HYNIC-TFA TGA curve, the weight-loss values were obtained in four phases, highlighting the conjugated events that occurred between the temperatures of 117–303.44 °C and 303.44–423 °C, which represented a loss that totaled 64.91% of the total sample mass. According to the characteristics of the thermograms, it was possible to draw a profile of thermal degradation between the samples and determine if there was an increase in thermal stability after the functionalization process.

Considering a fixed point of residual mass for all thermograms (30%), it was possible to make a comparison between the temperatures identified at each point of the studied samples. In view of this information, it was possible to observe that the nanocellulose sample reached a residual mass value of 30% when the temperature reached 346 °C. As for the samples of HYNIC and NC-HYNIC-TFA, the same percentage of mass was only obtained when temperatures reached 330 °C and 397 °C, respectively. Therefore, it is possible to determine that after the process of functionalization of the NC with HYNIC, there was an increase in thermal stability, since a higher temperature was necessary to promote a reduction of mass correlated with the sample of NHS-HYNIC-TFA.

These characteristics can be easily observed when comparing the first two mass reduction events of thermograms 1 and 3 (Fig. 3). Thus, by comparing the NC-HYNIC-TFA and NC, the presence of the substituted groups on the NC skeleton is expected to influence the thermo-stability. The new decomposition temperatures of NC-HYNIC-TFA can be attributed to the presence of the new functionalities on the NC framework that can be due to the formation of a denser crystalline structure [69]. Furthermore, the higher thermal

stability of NC-HYNIC-TFA could be due to the smaller particle size and a higher ratio of particle surface than NC, which could correspond to the ultrasonication process [69, 70] and possibly to the new chemical bonds or adsorption process generated with the functionalization.

The chemical strategy of the radiolabeling via a renewable material such as NC allows us to generate potential imaging agents in cancer diagnosis. The radiolabeling of NC-HYNIC-TFA with ^{99m}Tc easily yielded a new radioactive product, in a short time (20 min), with low potential radiation exposure [45]. The study of radiochemical purity showed a high radiolabeling yield ($98 \pm 1.2\%$). In vitro studies revealed a good stability profile in the reaction milieu above 90% for at least 3 h. This new strategy of radiolabeled NC is a promising alternative platform for cancer molecular imaging.

Conclusions

In this work, we reported the successful utilization of cellulosic biomass from rice husk as a renewable source. NC material was prepared via eco-friendly enzymatic hydrolysis using *Trichoderma reseii* and *Phanaerochaete chrysosporium* via a semi-solid fermentation system, which resulted in an efficient yield of 55%. The NC prepared had an average size of 10 ± 4 nm and showed a morphology of laminar-like nanofibers. Furthermore, the renewable material NC-HYNIC-TFA was successfully synthesized, and it was possible to radiolabel it, revealing a high radiolabeling yield and high stability. The performance of this NC system is a sign of promising applications in radiodiagnosis as diagnostic probes. Future works will delve into the types of available bonds offered by nanocellulose and bond affinity.

Acknowledgements This work was supported by a scholarship ID 156 for Ph.D. student N.L from Comisión Sectorial de Investigación Científica (CSIC-Uruguay). The authors are grateful to Javier Villalobos and Sergio Paniagua for their technical support and useful discussions.

Funding The authors did not receive support from any organization for the submitted work.

Declarations

Conflict of interest The authors have no conflict of interest to declare that are relevant to the content of this article.

References

1. Rajinipriya, M., Nagalakshmaiah, M., Robert, M., Elkoun, S.: Importance of agricultural and industrial waste in the field of nanocellulose and recent industrial developments of wood-based nanocellulose: a review. ACS Sustain. Chem. Eng. **6**(3), 2807–2828 (2018)
2. Zhang, S., Zhang, F., Jin, L., Liu, B., Mao, Y., Liu, Y., Huang, J.: Preparation of spherical nanocellulose from waste paper by aqueous NaOH/thiourea. Cellulose **26**(8), 5177–5185 (2019)
3. Curvello, R., Raghuwanshi, V.S., Garnier, G.: Engineering nanocellulose hydrogels for biomedical applications. Adv. Coll. Interface. Sci. **267**, 47–61 (2019)
4. Hossain, M.I., Zaman, H., Rahman, T.: Derivation of nanocellulose from native rice husk. Chem. Eng. Res. Bull. **20**(1), 19 (2018)
5. Ravindran, R., Jaiswal, A.K.: Exploitation of food industry waste for high-value products. Trends Biotechnol. **34**(1), 58–69 (2016)
6. Fritsch, C., Staebler, A., Happel, A., Cubero, M.A., Aguiló-Aguayo, I., Abadias, M., Gallur, M., Cigognini, I.M., Montanari, A., López, M.J., Suárez-Estrella, F., Brunton, N., Luengo, E., Sisti, L., Ferri, M., Belotti, G.: Processing, valorization and application of bio-waste derived compounds from potato, tomato olive and cereals: a review. Sustainability. **9**, 1492 (2017)
7. Navarro, M.V., Vega-Baudrit, J.R., Sibaja, M.R., Melero, F.J.: Use of rice husk as filler in Flexible Polyurethane Foams. Macromol. Symp. **321**(1), 202–207 (2012)
8. Kumar, S., Sangwan, P., Dhankhar, R., Mor, V., Bidra, S.: Utilization of rice husk and their ash: a review. Res. J. Chem. Environ. Sci. **1**(5), 126–129 (2013)
9. Thompson, L., Azadmanjiri, J., Nikzad, M., Sbarski, I., Wang, J., Yu, A.: Cellulose nanocrystals: production, functionalization and advanced applications Rev. Adv. Mater. Sci. **58**, 1–16 (2019)
10. Mariño, M., Lopes da Silva, L., Durán, N., Tasic, L.: Enhanced materials from nature: nanocellulose from citrus waste. Molecules **20**(4), 5908–5923 (2015)
11. Vigneshwaran, N., Satyamurthy, P.: Nanocellulose production using cellulose degrading fungi, pp. 321–331. In Advances and Applications Through Fungal Nanobiotechnology. Springer, Cham (2016)
12. Phanthong, P., Reubroycharoen, P., Hao, X., Xu, G., Abudula, A., Guan, G.: Nanocellulose: extraction and application. Carbon Res. Conv. **1**(1), 32–43 (2018)
13. Lin, N., Dufresne, A.: Nanocellulose in biomedicine: current status and future prospect. Eur. Polymer J. **59**, 302–325 (2014)
14. Jorfi, M., Foster, E.J.: Recent advances in nanocellulose for biomedical applications. J. Appl. Polym. Sci. **132**(14), 41719 (2015)
15. de Oliveira, A.D., Gonçalves, C.A.: Polymer Nanocomposites with Different Types of Nanofiller. Sivasankaran, S., (Ed.) IntechOpen. (2019).
16. Dufresne, A., Castaño, J.: Polysaccharide nanomaterial reinforced starch nanocomposites: a review. Starch - Stärke. **69**(1–2), 1500307 (2016)
17. Bongao, H.C., Gabatino, R.R.A., Arias, C.F.H., Magdaluyo, E.R., Jr.: Micro/nanocellulose from waste Pili (*Canarium ovatum*) pulp as a potential anti-ageing ingredient for cosmetic formulations. Mater. Today: Proceed. **22**, 275–280 (2020)
18. Soccol, C., Ferreira, E., Junior, L., Grace, S., Lorenci, A., Porto, P.: Recent developments and innovations in solid state fermentation. Biotechnol. Res. Innov. **1**(1), 52–71 (2017)
19. Manan, M.A., Webb, C.: Design aspects of solid state fermentation as applied to microbial bioprocessing. J. Appl. Biotechnol. Bioeng. **4**(1), 511–532 (2017)
20. Lopretti, M., Lecot, N., Rodriguez, A., Lluberas, G., Orozco, F., Bolaños, L., Montes de Oca, G., Cerecetto, H., Vega-Baudrit, J.: Biorefinery of rice husk to obtain functionalized bioactive compounds. J. Renew. Mater. **7**(4), 313–324 (2019)
21. Owen, S.C., Chan, D.P.Y., Shoichet, M.S.: Polymeric micelle stability. Nano Today **7**(1), 53–65 (2012)
22. Lu, Y., Park, K.: Polymeric micelles and alternative nanonized delivery vehicles for poorly soluble drugs. Int. J. Pharm. **453**(1), 198–214 (2013)

23. Lecot, N., Glisoni, R., Oddone, N., Benech, J., Fernández, M., Gambini, J.P., Cabral, P., Sosnik, A.: Glucosylated polymeric micelles actively target curcumin to a breast cancer model. Adv. Ther. **2000010**, 1–10 (2020)
24. Ono, M., Arano, Y., Mukai, T., Fujioka, Y., Ogawa, K., Uehara, T., Saga, T., Konishi, J., Saji, H.: 99mTc-HYNIC-derivatized ternary ligand complexes for 99mTc-labeled polypeptides with low in vivo protein binding. Nucl. Med. Biol. **28**(3), 215–224 (2001)
25. García, M.F., Gallazzi, F., de Souza Junqueira, M., Fernández, M., Camacho, X., da Silva Mororó, J., Faria, D., de Godoi Carneiro, C., Couto, M., Carrión, F., Pritsch, O., Chammas, R., Quinn, T., Cabral, P., Cerecetto, H.: Synthesis of hydrophilic HYNIC-[1,2,4,5]tetrazine conjugates and their use in antibody pretargeting with 99m Tc. Organ. Biomol. Chem. **16**(29), 5275–5285 (2015)
26. Guleria, M., Das, T., Vats, K., Amirdhanayagam, J., Mathur, A., Sarmad, H.D., Dash, A.: Preparation and evaluation of 99mTc-labeled porphyrin complexes prepared using PNP and HYNIC cores: studying the effects of core selection on pharmacokinetics and tumor uptake in a mouse model. Med. Chem. Commun. **10**, 606–615 (2019)
27. Levente, K., Meszaros, A.D., Stefano, C.G., Biagini, Blower, P.J.: Hydrazinonicotinic acid (HYNIC) – Coordination chemistry and applications in radiopharmaceutical chemistry. Inorganica Chimica Acta. **363**(6), 1059–1069 (2010)
28. Torabizadeh, S.A., Abedi, S.M., Noaparast, Z., Hosseinimehr, S.J.: Comparative assessment of a 99m Tc labeled H12992-HYNIC peptide bearing two different co-ligands for tumor-targeted imaging. Bioorgan. Med. Chem. **25**(9), 2583–2592 (2017)
29. Liu, S.: 6-Hydrazinonicotinamide Derivatives as Bifunctional Coupling Agents for 99mTc-Labeling of Small Biomolecules. Contrast Agents III. Topics in Current Chemistry. 252. Springer, Berlin, Heidelberg.
30. Anzola, L.K., Rivera, J.N., Dierckx, R.A., Lauri, C., Valabrega, S., Galli, F., Moreno, S., Glaudemans, A.W.J., Signore, A.: Value of somatostatin receptor scintigraphy with 99mTc-HYNIC-TOC in patients with primary sjögren syndrome. J. Clin. Med. **8**(6), 763 (2019)
31. Sarparanta, M., Pourat, J., Carnazza, K.E., Tang, J., Paknejad, N., Reiner, T., Kostiainen, M.A., Lewis, J.S.: Multimodality labeling strategies for the investigation of nanocrystalline cellulose biodistribution in a mouse model of breast cancer. Nucl. Med. Biol. **80–81**, 1–12 (2019)
32. Imlimthan, S., Otaru, S., Keinänen, O., Correia, A., Lintinen, K.S., Santos, H.A., Airaksinen, A.J., Kostiainen, M.A., Sarparanta, M.: Radiolabeled molecular imaging probes for the in vivo evaluation of cellulose nanocrystals for biomedical applications. Biomacromol **20**(2), 674–683 (2018)
33. Lopretti, M. Tesis de PhD en Biología 1990. Sistemas enzimáticos de hongos y bacterias modificadoras de Lignina, PEDECIBA, UdelaR.
34. Lopretti, M., Esquivel, M., Madrigal, S., Corrales, Y., Vega-Baudrit, J.R.: Preliminary study of the production of hybrid compounds of chitosan and polyphenols derived from lignin from agroindustry and shrimp fishery. Revista Científica. 27(1) (2017).
35. Tappi Standards, T203 OS-61. Technical Association of the Pulps and Paper Industry, 360 Lexington Avenue, New York, NY 10017. https://research.cnr.ncsu.edu/wpsanalytical/documents/T203.PDF. Accessed 3 Nov 2020.
36. Martelli-Tosi, M., Masson, M.M., Silva, N.C., Esposto, B.S., Barros, T.T., Assis, O.B., Tapia-Blácido, D.R.: Soybean straw nanocellulose produced by enzymatic or acid treatment as a reinforcing filler in soy protein isolate films. Carbohyd. Polym. **198**, 61–68 (2018)
37. Leung, A.C.W., Hrapovic, S., Lam, E., Liu, Y., Male, K.B., Mahmoud, K.A., Luong, J.H.T.: Characteristics and properties of carboxylated cellulose nanocrystals prepared from a novel one-step procedure. Small **7**(3), 302–305 (2011)
38. Navarro, J.R.G., Bergström, L.: Labelling of N-hydroxysuccinimide-modified rhodamine B on cellulose nanofibrils by the amidation reaction. RSC Adv. **4**(105), 60757–60761 (2014)
39. Navarro, J.R.G., Conzatti, G., Yu, Y., Fall, A.B., Mathew, R., Eden, M., Bergström, L.: Multi-color fluorescent labelling of cellulose nanofibrils by click-chemistry. Biomacromol **16**, 1293–1300 (2015)
40. Wei, L., Agarwal, U.P., Hirth, K.C., Matuana, L.M., Sabo, R.C., Stark, N.M.: Chemical modification of nanocellulose with canola oil fatty acid methyl ester. Carbohyd. Polym. **169**, 108–116 (2017)
41. Wu, W., Song, R., Xu, Z., Jing, Y., Dai, H., Fang, G.: Fluorescent cellulose nanocrystals with responsiveness to solvent polarity and ionic strength. Sens. Actuators, B Chem. **275**, 490–498 (2018)
42. Hu, Z., Zhai, R., Li, J., Zhang, Y., Lin, J.: Preparation and Characterization of Nanofibrillated Cellulose from Bamboo Fiber via Ultrasonication Assisted by Repulsive Effect. Int. J. Polym. Sci. 1–9 (2017).
43. Szymańska-Chargot, M., Cieśla, J., Chylińska, M.: Effect of ultrasonication on physicochemical properties of apple based nanocellulose-calcium carbonate composites. Cellulose **25**, 4603–4621 (2018)
44. Garcia, M.F., Calzada, V., Camacho, X., Goicochea, E., Gambini, J.P., Quinn, T.P., Porcal, W., Cabral, P.: Microwave-assisted Synthesis of HYNIC Protected Analogue for 99mTc Labeled Antibody. Current Radiopharmaceuticals. 7(2) (2014).
45. Oda, C.M.R., Fernandes, R.S., de Araújo Lopes, S.C.: Synthesis, characterization and radiolabeling of polymeric nano-micelles as a platform for tumor delivering. Biomed. Pharmacother. 89:268–275 (2017).
46. Ocampo-García, B.E., Ramírez, F.M., Ferro-Flores, G., De. León-Rodríguez, L.M., Santos-Cuevas, C.L., Morales-Avila, E., de Murphy, C.A., Pedraza-López, M., Medina, L.A., Camacho-López, M.A.: (99m) Tc-labelled gold nanoparticles capped with HYNIC-peptide/mannose for sentinel lymph node detection. Nucl. Med. Biol. **38**(1), 1–11 (2011)
47. Monteiro, LOF., Fernandes, RS, Castro LC, Valbert N. Cardoso, Mônica C. Oliveira, Danyelle M. Townsend, Alice Ferretti, Domenico Rubellod, Elaine A. Leitea, André L.B. de Barros.: Technetium-99m radiolabeled paclitaxel as an imaging probe for breast cancer in vivo. Biomed Pharmacother. 89, 146–151 (2017).
48. Cabrera M, Medrano, A., Lecot, N., Fernandez, M., Moreno, M., Chabalgoity, J.A., Gambini, J.P., Alonso, O., Balter, H., Cabral, P.: A novel method to radiolabel stealth liposome through 1,2-dimyristoyl-sn-glycero-3-phosphoethanolamine-N-DTPA with 99mTc and biological evaluation. J. Anal. Oncology. 1 (2013).
49. Camacho, X., Garcia, M.F., Calzada, V., Fernandez, M., Porcal, W., Alonso, O., Gambini, J., Cabral, P.: Synthesis and evaluation of 99mTc chelate-conjugated bevacizumab. Curr. Radiopharm. **6**(1), 12–19 (2013)
50. Tejería, E., Giglio, J., Fernández, L., Rey, A.: Development and evaluation of a 99mTc(V)-nitrido complex derived from estradiol for breast cancer imaging. Appl. Radiat. Isotopes. 154, 108854 (2019).
51. Wandas, M., Puszko, A.: The IR spectra of 2-alkylamino- and alkylnitramino-3- or 5-nitro-4-methylpyridine derivatives. Chem. Heterocycl. Compd. **36**, 796–800 (2000)
52. Hossain, S.S., Mathur, L., Roy, P.K.: Rice husk/rice husk ash as an alternative source of silica in ceramics: a review. J. Asian Ceram. Soc. **6**(4), 299–313 (2018)
53. Ribeiro, R.S., Pohlmann, B.C., Calado, V., Bojorge, N., Pereira, N., Jr.: Production of nanocellulose by enzymatic hydrolysis: Trends and challenges. Eng. Life Sci. **19**(4), 279–291 (2019)
54. Satyamurthy, P., Jain, P., Balasubramanya, R.H., Vigneshwaran, N.: Preparation and characterization of cellulose nanowhiskers

from cotton fibres by controlled microbial hydrolysis. Carbohyd. Polym. **83**(1), 122–129 (2011)
55. Satyamurthy, P., Vigneshwaran, N.: A novel process for synthesis of spherical nanocellulose by controlled hydrolysis of microcrystalline cellulose using anaerobic microbial consortium. Enzyme Microb. Technol. **52**(1), 20–25 (2013)
56. Li, X., Kondo, R., Sakai, K.: In vivo and in vitro biobleaching of unbleached hardwood kraft pulp by a marine fungus, Phlebia sp. MG-60. Progress Biotechnol **21**, 185–191 (2002)
57. Nunes, C. S., Malmlöf, K.: Enzymatic decontamination of antimicrobials, phenols, heavy metals, pesticides, polycyclic aromatic hydrocarbons, dyes, and animal waste. Enzymes Human Animal Nutr. (pp. 331–359). Academic Press. (2018).
58. Chowdhary, P., More, N., Yadav, A., Bharagava, R. N.: Ligninolytic Enzymes: An Introduction and Applications in the Food Industry. In Enzymes in Food Biotechnology (pp. 181–195). Academic Press. (2019).
59. De. Aguiar, J., Bondancia, T.J., Claro, P.I.C., Mattoso, L.H.C., Farinas, C.S., Marconcini, J.M.: Enzymatic deconstruction of sugarcane bagasse and straw to obtain cellulose nanomaterials. ACS Sustain. Chem. Eng. **8**, 2287–2299 (2020)
60. Habibi, Y.: Key advances in the chemical modification of nanocelluloses. Chem. Soc. Rev. **43**(5), 1519–1542 (2014)
61. Wang, Y., Wang, X., Xie, Y.: Functional nanomaterials through esterification of cellulose: a review of chemistry and application. Cellulose **25**, 3703–3731 (2018)
62. Dien, L. Q., Cuong, T. D., Minh Phuong, N. T., Hoang, P. H., Truyen, D. N., Minh Nguyet, N. T.: Nanocellulose fabrication from *Oryza sativa* L. rice straw using combined treatment by hydrogen peroxide and dilute sulfuric acid solution. Energy Sources, Part A: Recovery, Utilization, and Environmental Effects. 1–10 (2019).
63. Onkarappa, H. S., Prakash, G. K., Pujar, G. H., Rajith Kumar, C. R., Betageri, V. S.: Facile synthesis and characterization of nanocellulose from *Zea mays* husk. Polym. Comp. 1 (7) (2020).
64. Rajinipriya, M., Nagalakshmaiah, M., Robert, M., Elkoun, S.: Importance of agricultural and industrial waste in the field of nanocellulose and recent industrial developments of wood based nanocellulose: a review. ACS Sustain. Chem. Eng. **6**, 2807–2828 (2018)
65. Michelin, M., Gomes, D.G., Romaní, A., Polizeli, M.D.L., Teixeira, J.A.: Nanocellulose production: exploring the enzymatic route and residues of pulp and paper industry. Molecules **25**(15), 3411 (2020)
66. Csiszar, E., Kalic, P., Kobol, A., Ferreira, E.P.: The effect of low frequency ultrasound on the production and properties of nanocrystalline cellulose suspensions and films. Ultrason. Sonochem. **31**, 473–480 (2016)
67. Ludueña, L., Fasce, D., Alvarez, V.A., Stefani, P.M.: Nanocellulose from rice husk following alkaline treatment to remove silica. BioResources **6**(2), 1440–1453 (2011)
68. Abraham, E., Thomas, M.S., John, C., Pothen, L.A., Shoseyov, O., Thomas, S.: Green nanocomposites of natural rubber/nanocellulose: membrane transport, rheological and thermal degradation characterisations. Ind. Crops Prod. **51**, 415–424 (2013)
69. Barbash, V.A., Yashchenko, O.V., Vasylieva, O.A.: Preparation and Properties of Nanocellulose from Miscanthus x giganteus. J. Nanomater. 3241968 (2019).
70. Edi Syafri, S., Mashadi, E.Y., Deswitab, M.A., Hairul Abral, S.M., Sapuane, R.A., Ilyas, A.F.: Effect of sonication time on the thermal stability, moisture absorption, and biodegradation of water hyacinth (*Eichhornia crassipes*) nanocellulose-filled bengkuang (*Pachyrhizus erosus*) starch biocomposites. J. Mater. Res. Technol. **8**(6), 6223–6231 (2019)

Authors and Affiliations

Lecot Nicole[1] · Gandaras Rosario[1,2] · Batista-Menezes Diego[3] · Montes de Oca-Vásquez Gabriela[3] · Cabral Pablo[4] · García Ma. Fernanda[4] · Vega-Baudrit José[3,5] · Cerecetto Hugo[2,4] · Lopretti Mary[1]

✉ Lecot Nicole
nlecot@fcien.edu.uy

[1] Laboratorio de Técnicas Nucleares Aplicadas a la Bioquímica y Biotecnología, Centro de Investigaciones Nucleares, Facultad de Ciencias, Universidad de la República, Montevideo, Uruguay

[2] Grupo de Química Orgánica Medicinal, Facultad de Ciencias, Instituto de Química Biológica, Universidad de la República, Montevideo, Uruguay

[3] National Nanotechnology Laboratory, National Center for High Technology, 10109 Pavas, San José, Costa Rica

[4] Laboratorio de Radiofarmacia, Centro de Investigaciones Nucleares, Facultad de Ciencias, Universidad de la República, Montevideo, Uruguay

[5] Laboratory of Polymer Science and Technology, School of Chemistry, Universidad Nacional, Omar Dengo Campus, 86-3000 Heredia, Costa Rica